

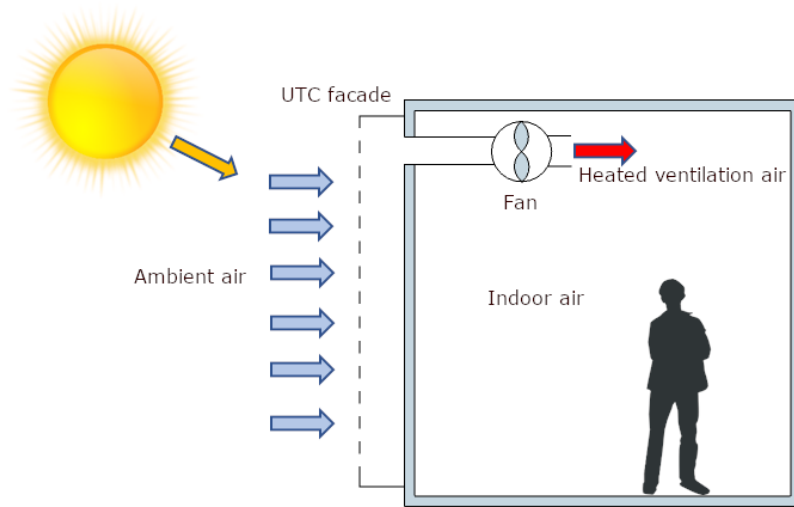
25 In recent years, the performance of active building façades has been widely studied, especially those
26 façades in which the use of renewable energy sources reduces the building energy consumption.
27 Unglazed transpired collector (UTC) façades can provide ventilation preheating in the winter and
28 night free cooling in the summer (Peci et al. 2019; Kassai et al. 2018). Unlike other more sophisticated
29 systems, this is an inexpensive and minimally invasive solution for refurbishment of the façades of
30 existing buildings. A UTC façade consists of a perforated metal layer that absorbs solar radiation, an
31 air plenum and an insulation layer, which may be the existing façade of the building. Ventilation air
32 is heated as it passes through the holes in the solar absorber layer and then is introduced into the
33 building, figure 1. In this way, the thermal boundary layer is sucked into the air plenum and the heat
34 loss to the exterior is minimised. The absorber layer should be painted in a dark colour with high solar
35 radiation absorptance and preferably with a low long wave emissivity, (Hall and Blower 2016). Due
36 to the constructive characteristics of this system, in some cases, the refurbishment of the façade
37 would only need the installation of the absorber layer and the ventilation system, or the connection
38 with the existing HVAC system (Badescu et al. 2019).

39 UTC façades have been installed in new and refurbished buildings for decades (Hollick 1996; Brown
40 et al. 2014; Al-damook and Khalil 2017; Fleck, Meier, and Matovic 2002). They have also been used
41 for industrial processes like crop drying or venting of livestock barns (Cordeau and Barrington 2011;
42 Love et al. 2014). Furthermore, they can be used for cooling when combined with other systems,
43 such as absorption or desiccant cooling systems, (Pesaran and Wipke 1994), (Peci, Comino, and Ruiz
44 de Adana 2018). Energy saving was achieved in all cases, although the efficiency varied according to
45 the weather conditions, especially wind velocity. However, there is still a lack of field measurements
46 to quantify the actual energy saving under ambient weather conditions.

47 The efficiency and feasibility of UTC façades have been studied by several authors (Collins and
48 Abulkhair 2014). On the one hand, the heat loss to the exterior due to natural convection, that could
49 be the main drawback of this system, has been found to be negligible, (Kutscher, Christensen, and
50 Barker 1993). On the other hand, one of the most influential variables on the performance of a UTC
51 was found to be the wind velocity and many authors concluded that this affects the efficiency of the
52 UTC as a solar collector (Al-damook and Khalil 2017; Fleck, Meier, and Matovic 2002; Vasan and
53 Stathopoulos 2014). Due to the variety of weather conditions during a season, an estimation of the
54 efficiency should consider the values over an extended period, and there is a lack of experimental
55 data in the literature with respect to this. This study supports theoretical and experimental research
56 by providing experimental evidence of the performance of the system.

57 In this study, the ventilation temperature was controlled using an on/off control strategy to prevent
58 cold air from entering the building. A similar control strategy was proposed by (Moon et al. 2017;
59 Gagliano, Aneli, and Nocera 2019; Giovanardi et al. 2015).

60 This study proposes a modular approach. A prototype of a UTC module was built and installed on the
61 façade of a test cell under ambient weather conditions in Cordoba, Spain. The effect of ambient
62 temperature and solar radiation on its performance was studied, and the values of the COP,
63 effectiveness, efficiency and temperature increase over almost one month were analysed. With the
64 data obtained, a case study was carried out to estimate the ventilation and ventilation heating energy
65 consumption savings. The aim of this study was to characterise the UTC module prototype behaviour
66 using experimental data measured over a period and to assess the feasibility of its installation to
67 refurbish a residential building in this location based on the experimental results.



68

69

Figure 1. Schematic of a UTC facade system

70

71 **Nomenclature:**

72 A_c UTC collector surface area (m²)

73 C_p Specific heat of air (J/kg K)

74 COP Coefficient of performance

75 \dot{E}_v Ventilation sensible heat load (W)

76 I_T Total irradiance on the collector (W/m²)

77 \dot{m} Air mass flow rate (kg/s)

78 $\dot{Q}_{conv,ext}$ Convection heat transfer rate from the collector to the ambient air (W)

79 $\dot{Q}_{conv,int}$ Convection heat transfer rate from the collector to the plenum air (W)

80 $\dot{Q}_{conv,sw}$ Convection heat transfer rate from the insulation panel to the plenum air (W)

81 \dot{Q}_{rad} Energy rate absorbed by the collector surface by radiation (W)

82 $\dot{Q}_{rad,long,ext}$ Long wave radiation interchange between the collector and the surroundings (W)

83 $\dot{Q}_{rad,long,int}$ Long wave radiation interchange between the collector and the insulation panel (W)

84 t_{on} Daily time with the fan running (s)

85 T_{amb} Ambient temperature (K)

86 T_{col} Collector surface temperature (K)

87 T_i Indoor temperature (K)

88	T_{out}	Collector outlet air temperature (K)
89	T_p	Plenum air temperature (K)
90	V_r	Daily ventilation air volume required by regulations (m ³)
91	\dot{W}_{fan}	Power consumption of the fan (W)
92	ε_{HX}	Collector effectiveness
93	η_{col}	Collector efficiency
94	ρ	Air density (kg/m ³)

95

96 **2. Methodology**

97

98 **2.1 Experimental set up**

99

100 A prototype of a UTC façade module was installed in a test cell under exterior weather conditions in
 101 Cordoba, south of Spain, coordinates 37°54'51.19"N 4°43'34.8"W. This location corresponds to a
 102 typical continental climate with mild winters and many sunny days, and therefore can be considered
 103 suitable for installing any kind of solar collector system. The façade was oriented to the south and
 104 there were no obstacles to the beam solar radiation nearby. The system was monitored in order to
 105 measure the temperatures of the different layers and the inlet air, the ventilation heat transfer rate
 106 to the cell and the main weather variables.

107

108 The experimental set up was used in a previous study (Peci et al. 2019). This set up consists of a
 109 modular site office of 6x2x2,5 m with a 3 cm sandwich panel cladding, see figure 2. The cell remained
 110 closed during the experiments, although leakage through cracks around the door and a small window
 111 existed. The air temperature inside the cell was kept within a normal range using an electric heater
 112 and an air conditioning system, with a set temperature of 23 °C. Figure 3 shows the position of the
 113 measurement probes. Temperatures were measured at three different heights for the four layers of
 114 the façade. The global solar radiation on the façade plane was measured using an analogue second
 115 class (<1.8%) pyranometer SR05-A1 installed on the façade itself. The ambient temperature was
 116 measured in a shielded case to avoid any solar radiation influence.

117

118

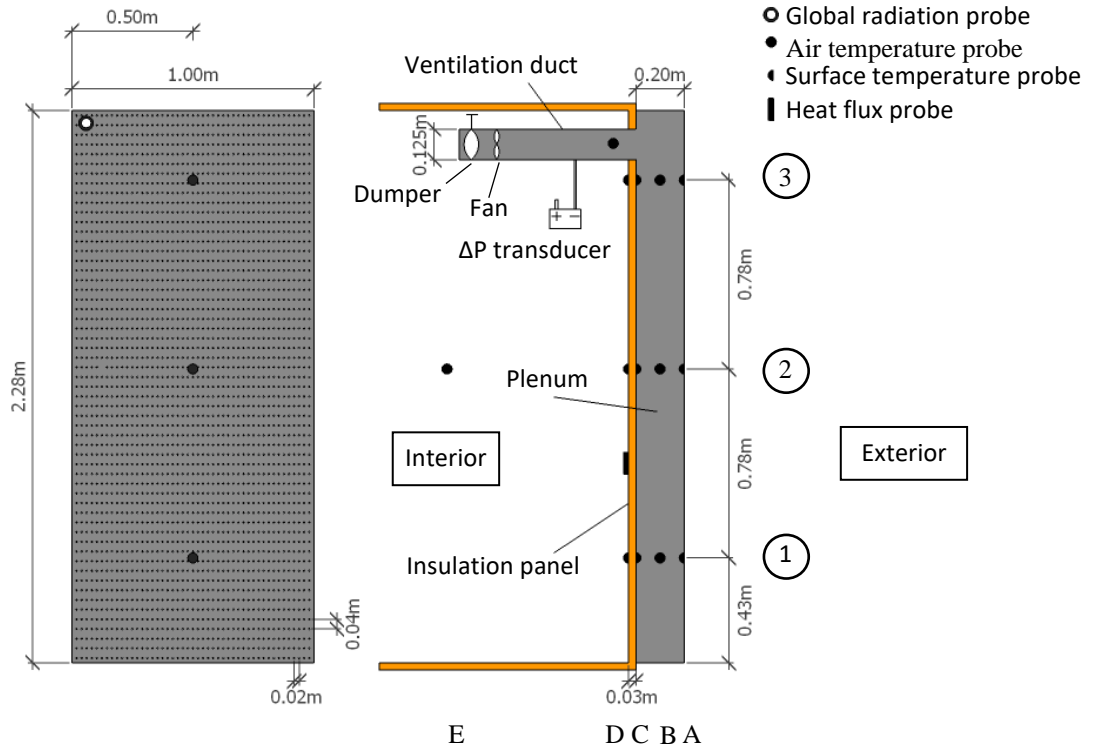
119



120
121

122 *Figure 2. The test cell with the position of the UTC façade module and the protected ambient temperature probe (right).*

123



124

125 *Figure 3. UTC experimental module dimensions and temperature probe locations. Probes were installed at three heights*
 126 *(1,2 and 3) in the steel plate (A), the plenum (B), the outer sandwich panel surface (C) and the inner sandwich panel*
 127 *surface (D).*

128

129 The UTC fan was controlled throughout a hysteresis cycle. It was automatically turned on when the
 130 inlet air temperature was above 23 °C and turned off when this temperature was below 21 °C. When
 131 the fan was on, the average air flow rate was constant with a value of 220 m³ h⁻¹. The suction velocity
 132 for this flow rate was 0.027 m/s. The average electric power consumption of the fan was 34 W.
 133 Further information about the experimental set up can be found in (Peci et al. 2019).

134

135 2.2 Theoretical model

136

137 A theoretical model based on energy balance equations was used to analyse the UTC façade
 138 performance. The energy balance in the collector surface, equation 1, and the overall energy balance,
 139 equation 2, gives the net energy entering the building (Leon and Kumar 2007).

140

$$141 \quad \dot{Q}_{rad} = \dot{Q}_{conv,ext} + \dot{Q}_{conv,int} + \dot{Q}_{rad,long,ext} + \dot{Q}_{rad,long,int} \quad (1)$$

$$142 \quad \dot{m}C_p(T_{out} - T_{amb}) = \dot{Q}_{conv,int} - \dot{Q}_{conv,sw} \quad (2)$$

143

144 The ventilation sensible heat load of a building can be evaluated as the difference between the
 145 energy of the inlet and outlet air streams, equation 3.

146

$$147 \quad \dot{E}_v = \dot{m}C_p(T_i - T_{amb}) \quad (3)$$

148

149 Effectiveness and efficiency were assessed with equations 4 and 5. The temperature increase was
 150 evaluated using equation 6, (Leon and Kumar 2007). $\varepsilon_{HX} =$

$$151 \frac{T_p - T_{amb}}{T_{col} - T_{amb}} \quad (4)$$

152

$$153 \eta_{col} = \frac{\dot{m} C_p (T_{out} - T_{amb})}{I_T A_c} \quad (5)$$

154

$$155 \Delta T = T_{out} - T_{amb} \quad (6)$$

156

157 The coefficient of performance, COP, of the UTC collector can be evaluated with the equation 7.

158 The only energy consumption of the system was that of the fan motor.

159

$$160 COP = \frac{\dot{m} C_p (T_{out} - T_{amb})}{\dot{W}_{fan}} \quad (7)$$

161

162 2.3 Case study

163 A typical apartment consisting of a living room, three bedrooms and two bathrooms was considered
 164 to study the rate of ventilation and ventilation heating achieved by the UTC façade module. The
 165 ventilation requirements for this case according to regulations (“Código Técnico de La Edificación
 166 (CTE) Documento HS 3 - Calidad de Aire Interior” 2017) are listed in table 1. The total daily flow rate
 167 required was 3283 m³/day. The percentage of the daily required ventilation achieved, and the
 168 percentage of daily ventilation heating requirements covered with the UTC module tested were
 169 evaluated with equations 7 and 8, respectively. From these data the area of UTC modules needed in
 170 each case was calculated. The south façade length was 15 m with a height of 3.25 m. Windows
 171 covered 5.5 m² of the façade and the area available for installing UTC modules was 47 m².

172

$$173 \% \text{ Ventilation achieved} = \frac{\dot{m} t_{on}}{\rho V_r} \cdot 100 \quad (7)$$

174

175

$$176 \% \text{ Ventilation heating achieved} = \frac{\dot{m} C_p (T_{out} - T_{amb}) t_{on}}{\rho V_r C_p (T_i - T_{amb})} \cdot 100 \quad (8)$$

177

178

Table 1

Room	Ventilation requirements (m ³ /s)
Living room	0.010
Main bedroom	0.008
Bedrooms	0.008
Bathrooms	0.012

179

180

181

182

183 **3. Results and analysis**

184

185 **3.1 Hourly results**

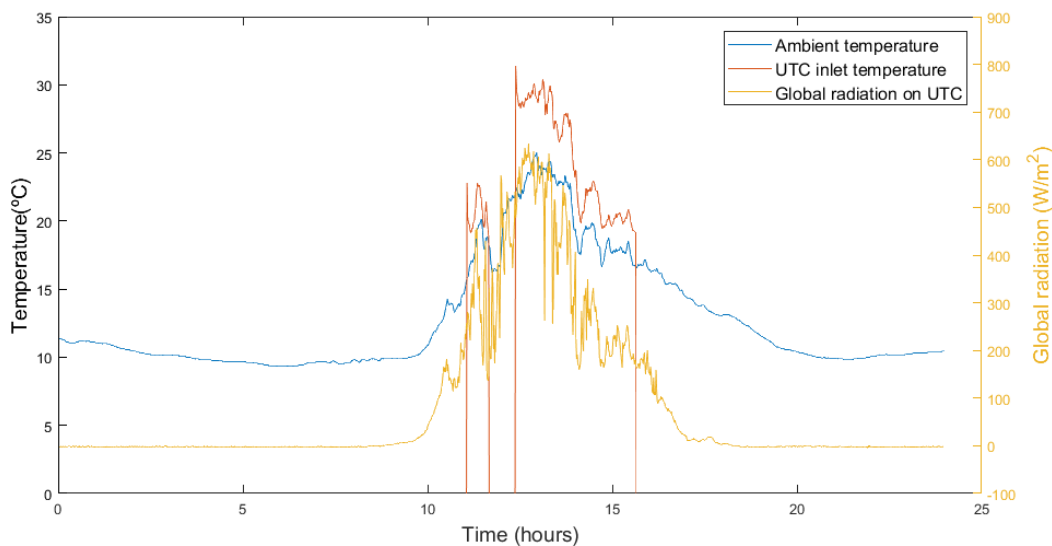
186 The typical behaviour of the UTC system during the day is shown in figures 4 to 7. They show the
187 experimental UTC outlet air temperatures for four typical days with combinations of high and low
188 global radiation and ambient temperature levels. The inlet air temperature is only represented when
189 the fan was on.

190 During the day shown in figure 4, despite the intermittent radiation levels on the façade, the
191 ventilation was running for most of the daytime, due to the high ambient temperatures. In the
192 midday periods, the temperature increase inside the UTC reached more than 5 °C, reaching maximum
193 values of about 30 °C. When there was not enough beam solar radiation, the ventilation was turned
194 off, so ventilation with low air temperature was not possible.

195 In the most unfavourable case, with cloudy sky and low temperatures, figure 5, the maximum UTC
196 outlet temperatures obtained were between 20 and 25 °C. The air flow rate was very intermittent,
197 only running when there was some beam solar radiation. During this kind of day, the UTC system was
198 not able to ventilate, as the temperature was not high enough to be introduced into the rooms.

199 As expected, UTC outlet temperatures increased with high global radiation on the façade. In the most
200 favourable case, figure 6, outlet air temperatures above 35 °C were measured. However, the inlet
201 temperature values were not as high as in the case when ambient temperature was low at the time
202 that solar radiation was high. For this case, high radiation and low ambient temperatures, figure 7,
203 maximum inlet temperatures between 25 °C and 30 °C were measured.

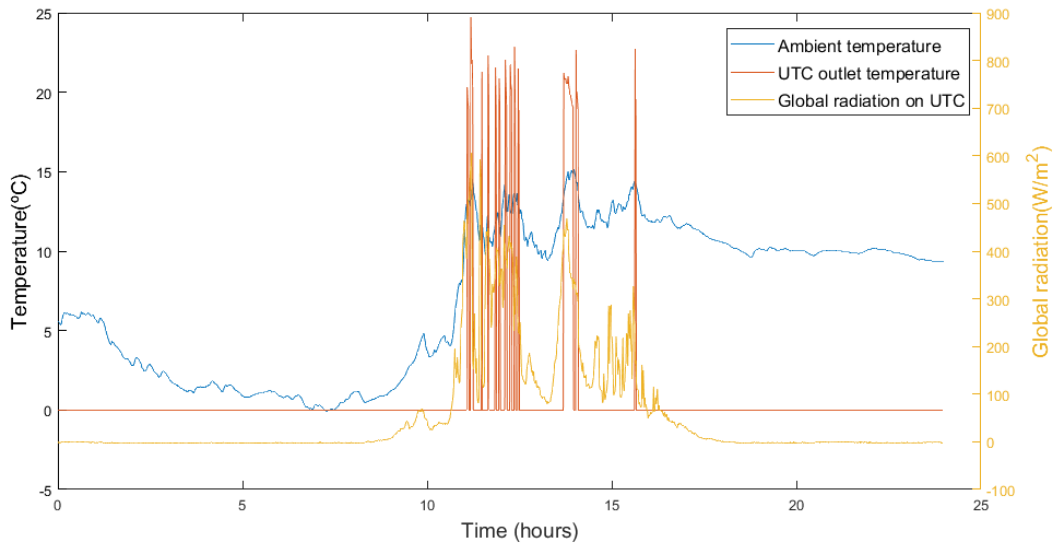
204



205

206

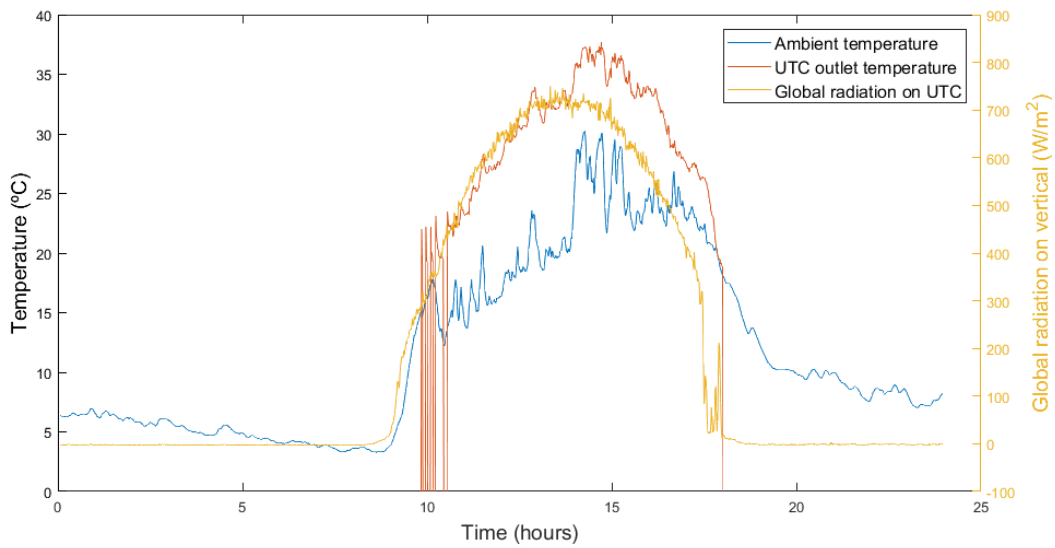
Figure 4. Measurements over a typical day with low radiation and high temperature levels.



207

208

Figure 5. Measurements over a typical day with low radiation and low temperature levels.



209

210

Figure 6. Measurements over a typical day with high radiation and high temperature levels.

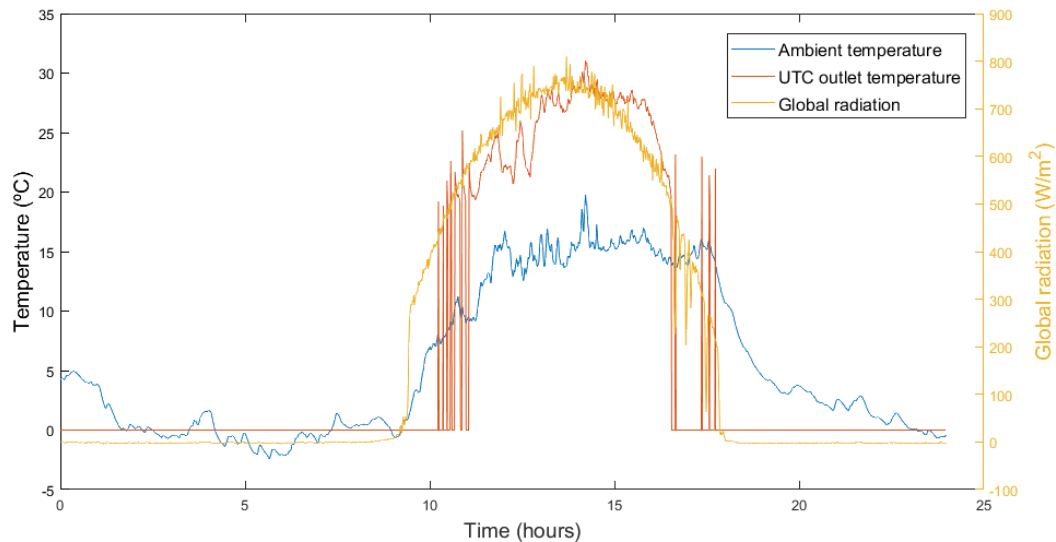


Figure 7. Measurements over a typical day with high radiation and low temperature levels.

211

212

213

214 According to these data, the more days with high solar radiation, the more heating energy saving will
 215 be obtained. Therefore, locations with many hours of beam solar radiation and low ambient
 216 temperature would benefit more from installing a UTC façade for heating. During cloudy days there
 217 would not be any ventilation, or the ventilation heat load would be higher if a ventilation system
 218 were working in the building. In any case, the installation of a UTC façade system does not imply an
 219 increase in the heating loads. In the experimental tests there were more days like those shown in
 220 figures 6 and 7.

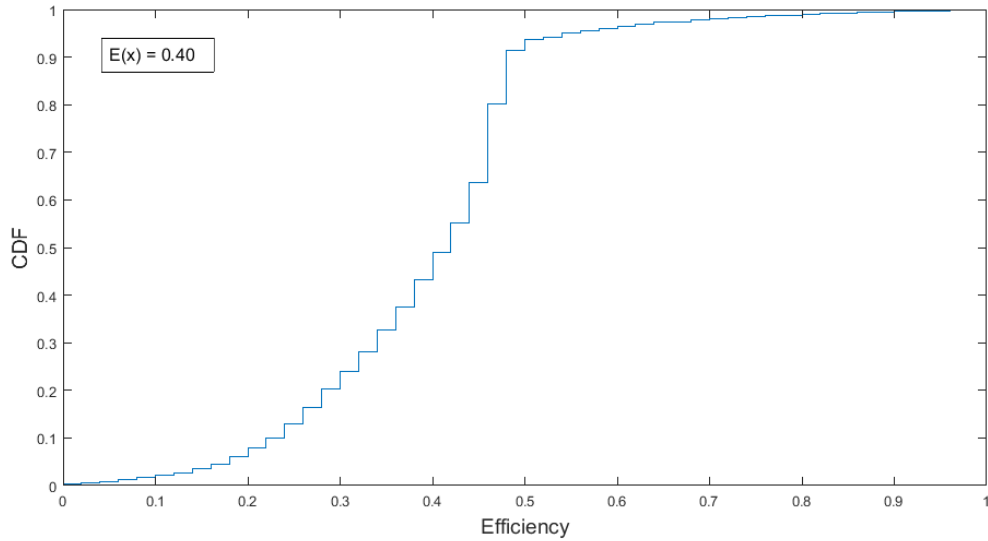
221

222

223 3.2 Efficiency and Effectiveness

224 The cumulative distribution function (CDF) of UTC efficiency and effectiveness measured during the
 225 test are represented in figures 8 and 9. The efficiency mean value was 0.40 and 90% of the efficiency
 226 values were found to be 0.46 or less. Effectiveness was found to be greater than 0.48 for 90% of the
 227 measurements, with a mean value of 0.52. The CDF of the effectiveness became steeper from values
 228 around 0.30, and it can be seen that 90 % of the effectiveness values fall between 0.30 and 0.60. The
 229 values of efficiency were more spread, with 90 % of the values between 0.21 and 0.48.

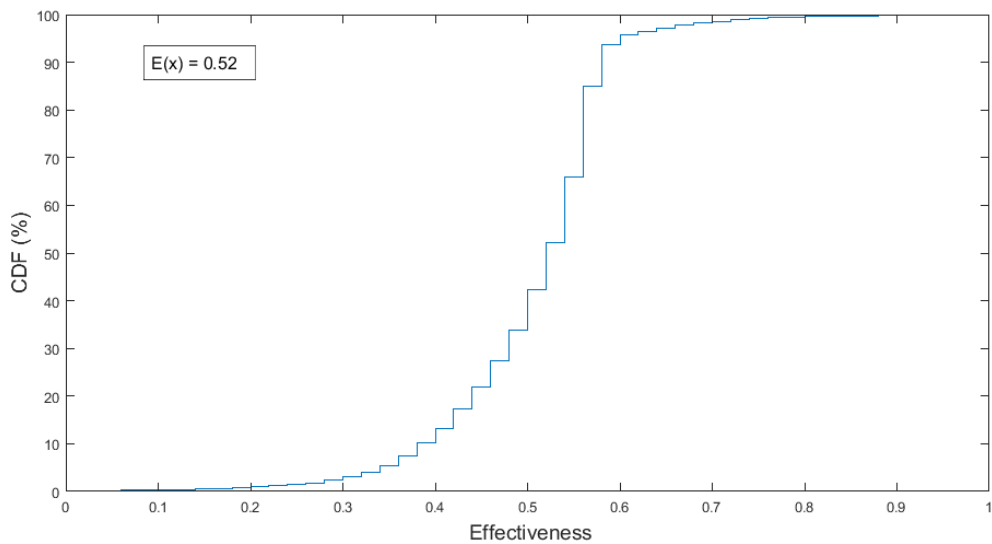
230 The values of efficiency and effectiveness obtained are in agreement with those found in literature.
 231 In (Collins and Abulkhair 2014), a comparison between numerical analysis and the results of other
 232 authors was carried out. In this study, values of effectiveness between 0.6 and 0.8 were found for a
 233 suction velocity of 0.027 m/s. Other authors, (Van Decker, Hollands, and Brunger 2001), found
 234 numerical and experimental values in the same range. Values of efficiency between 0.20 and 0.75
 235 were found in (Badache, Hall, and Rouse 2012) for high and low levels of absorptance, irradiation
 236 and flow rate.



237

238

Figure 8. Cumulative distribution function of the UTC module efficiency.



239

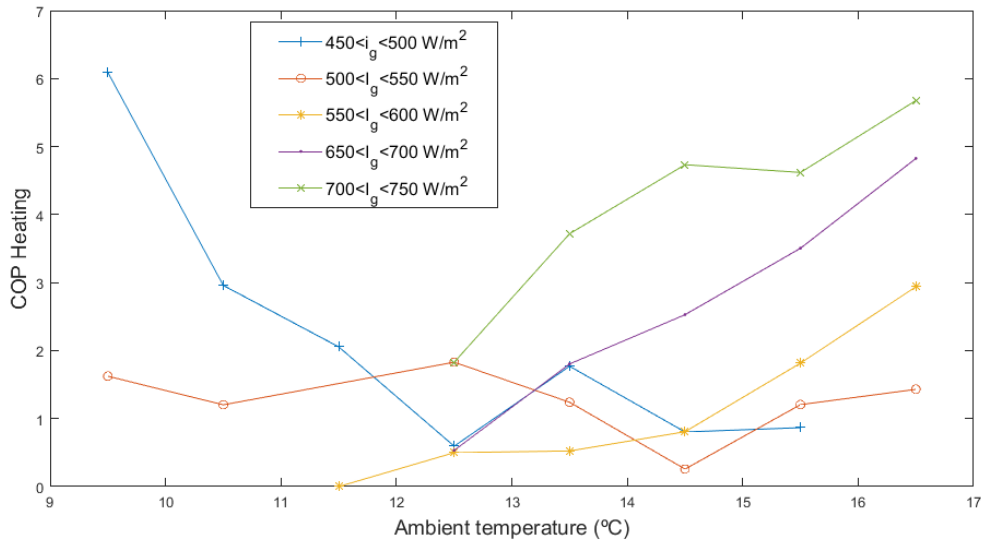
240

Figure 9. Cumulative distribution function of the UTC module effectiveness

241 From these results it can be concluded that, given the high dispersion of both efficiency and
 242 effectiveness, which is dependent on the weather variables, the study of the energy savings for a
 243 specific building should take into account the typical climate of its location. The effects of the weather
 244 variables on the performance of the UTC façade are analysed in the followig paragraphs.

245

246 **3.3 Effect of weather variables**



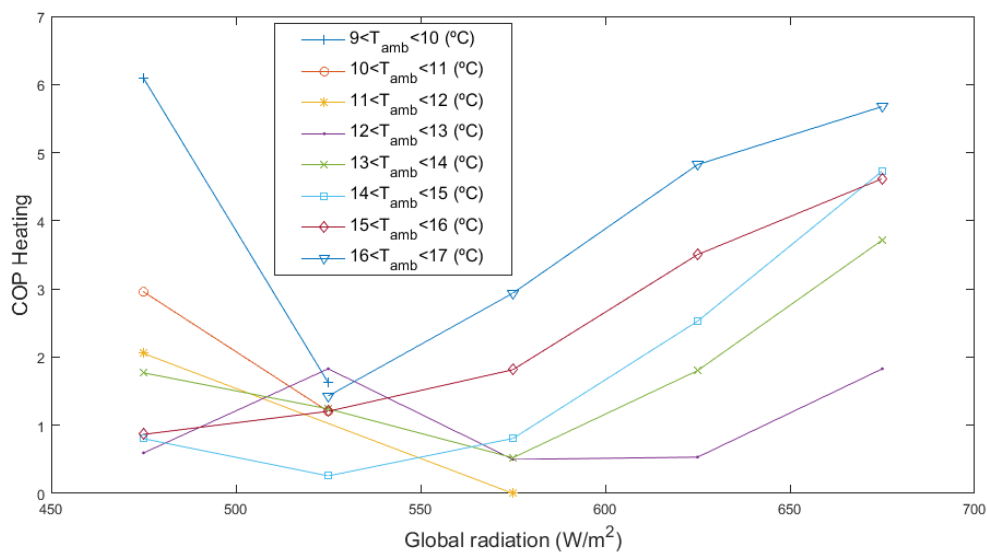
247

248

Figure 10. Variation of COP heating values with ambient temperature for different intervals of solar radiation.

249 Figure 10 shows the variation of heating COP with ambient temperature for different intervals of
 250 solar radiation on the collector. It can be seen that for the lowest radiation level COP decreased when
 251 the temperatures were below 13 °C. For the same range of temperatures, COP remained between
 252 0.5 and 1.8 when irradiation was between 500 and 550 W/m². When irradiation was higher than 550
 253 W/m² there was a clear trend for the COP to increase as ambient temperature increased.

254 Figure 11 shows the variation of heating COP with solar irradiation for several intervals of ambient
 255 temperature. It can be seen that there was a clear increasing trend of the COP for all the ambient
 256 temperature levels when global radiation was above 575 W/m². This highlights the importance of
 257 solar radiation on the performance of the UTC façade. However, COP increased for global radiation
 258 below 525 W/m² for ambient temperatures below 12 °C, where a small temperature increase has a
 259 considerable impact on the COP. Low radiation values usually corresponded to lower temperatures
 260 during the day, so the temperature increase was higher compared to those days with higher solar
 261 radiation.



262

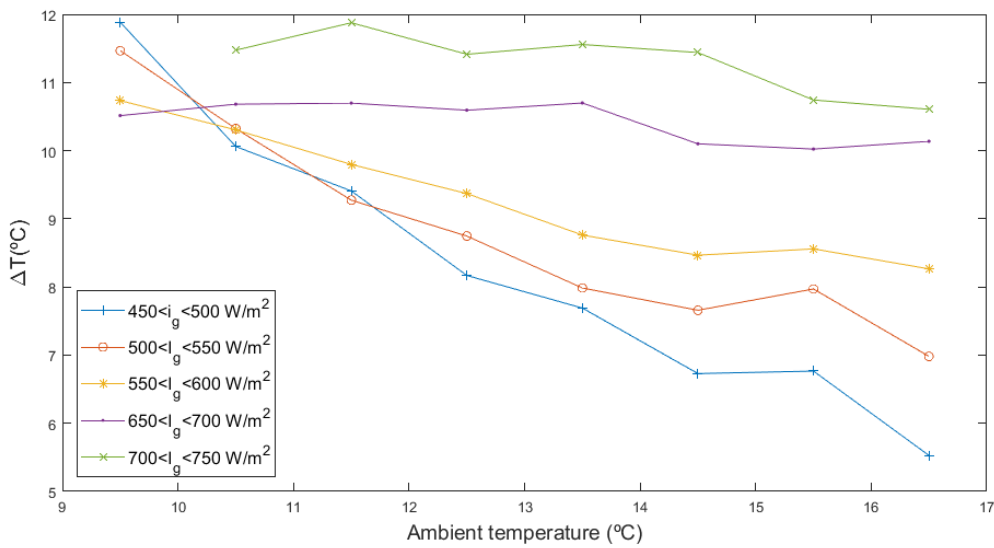
263

Figure 11. Variation of heating COP with global radiation on the UTC façade for several intervals of ambient temperature.

264 The effect of ambient temperature on the inlet air temperature increment is represented in figure
 265 12. It can be seen that the higher the ambient temperature, the lower the temperature increase. This
 266 trend is more noticeable for the cases with lower solar radiation levels. When the radiation levels
 267 were low, the collector surface temperature can not reach high temperatures, so if the ambient
 268 temperatures are also high, the temperature increase can not be very high. Figure 13 shows the
 269 variation of the air temperature increase with global radiation for several temperature intervals. The
 270 temperature increase tended to increase as global solar radiation increased, as expected. However,
 271 for low temperatures the trend was the opposite. This may be due to increasing heat loss to the
 272 exterior when temperatures were low.

273

274

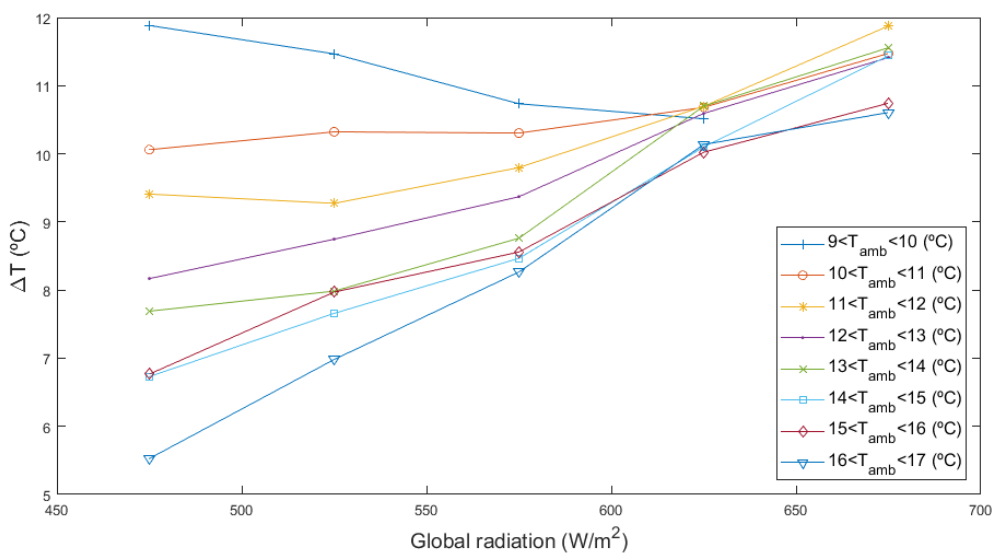


275

276

277

Figure 12. Variation of temperature increase in the UTC façade with ambient temperature for different solar irradiation intervals.



278

279

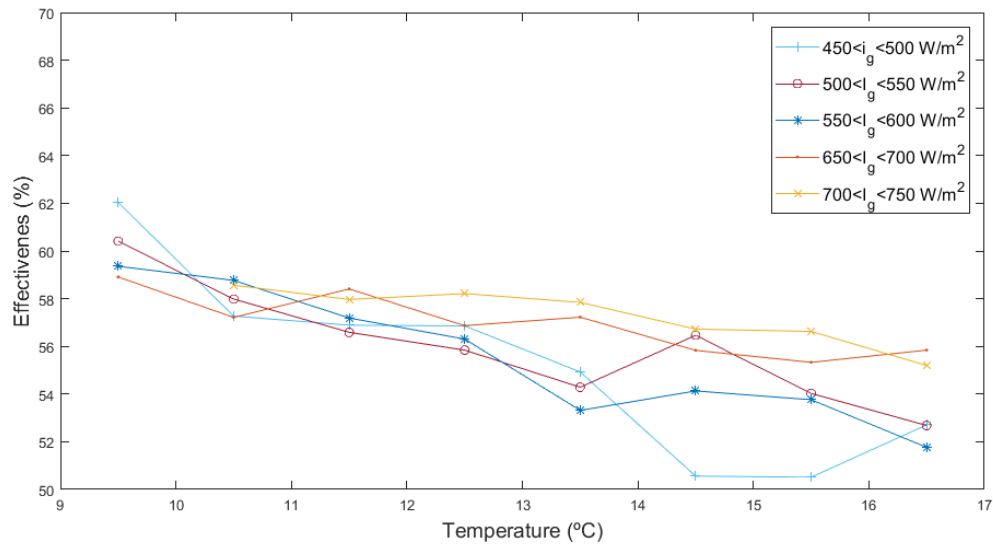
280

Figure 13. Variation of temperature increase in the UTC with global radiation for different ambient temperature intervals.

281 The variation of the effectiveness with ambient temperature is shown in figure 14. Effectiveness
 282 tended to decrease with temperature for all global radiation levels. As the ambient temperature
 283 increased, the temperature difference between the collector surface and the ambient air decreases,
 284 and the amount of energy transferred to the air was lower.

285 Figure 15 shows the variation of effectiveness with solar radiation for several ambient temperatures.
 286 The general trend for the effectiveness was to increase with solar radiation. However, for the lowest
 287 temperature levels this trend was the opposite. Again, this may be because of the increase of thermal
 288 loss to the exterior due to the low temperatures.

289

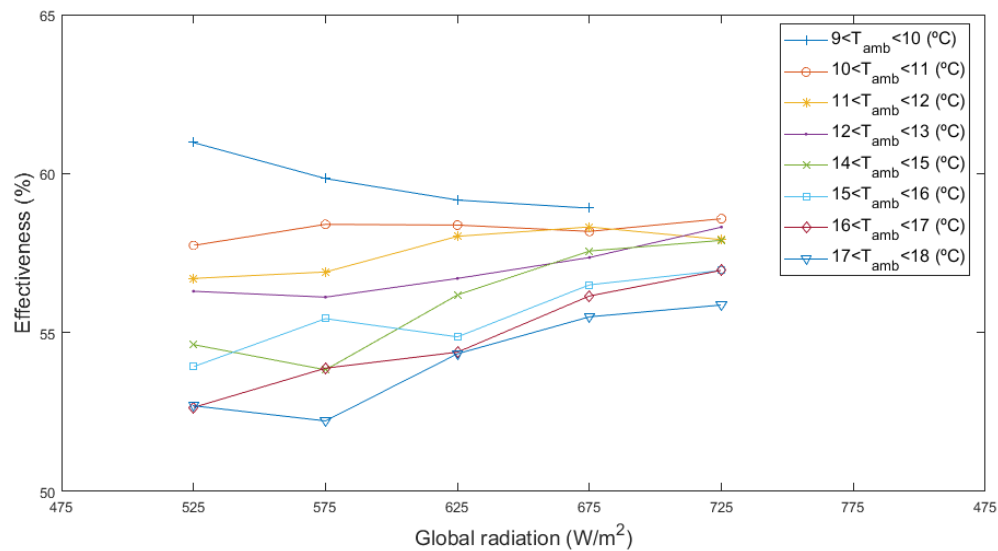


290

291

Figure 14. Variation of the effectiveness with ambient temperature for various global radiation intervals.

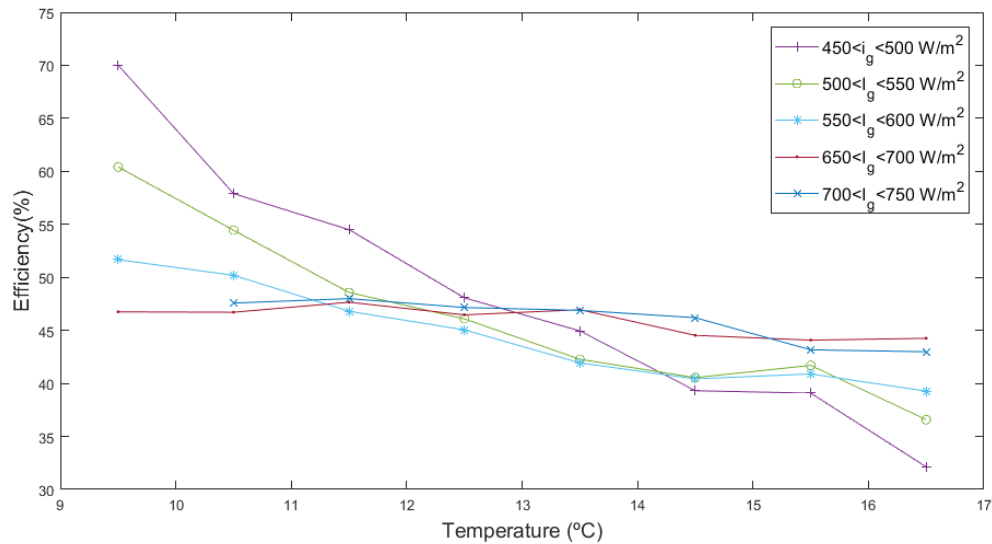
292



293

294

Figure 15. Variation of effectiveness with global radiation for different intervals of ambient temperature.



295

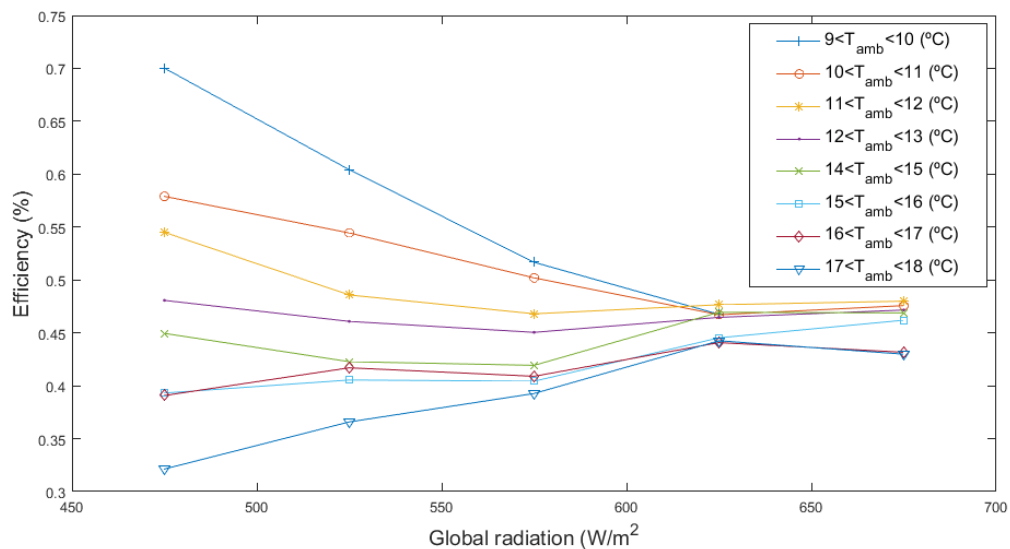
296

Figure 16. Variation of efficiency with ambient temperature for different intervals of global radiation.

297

Figure 16 shows the variation of the UTC efficiency with ambient temperature. Efficiency diminished with ambient temperature for every global radiation interval, and the decrement is higher for lower levels of solar radiation. The reason for this is that with high ambient temperatures, the temperature difference between ambient air and the collector decreases, and therefore convection heat transfer reduces. This effect was also pointed out in (Kutscher, Christensen, and Barker 1993). Regarding the dependence on solar radiation, figure 17 shows that efficiency values converge to a value between 0.4 and 0.5 for all ambient temperature intervals. For high solar radiation values, efficiency is independent of the ambient temperature. The decrease in the efficiency with high solar radiation was previously studied in (Fleck, Meier, and Matovic 2002), although the results were represented as a dispersion graph. Figure 17 shows that values are also ambient temperature dependent.

307



308

309

Figure 17. Variation of efficiency with global radiation for different intervals of ambient temperature.

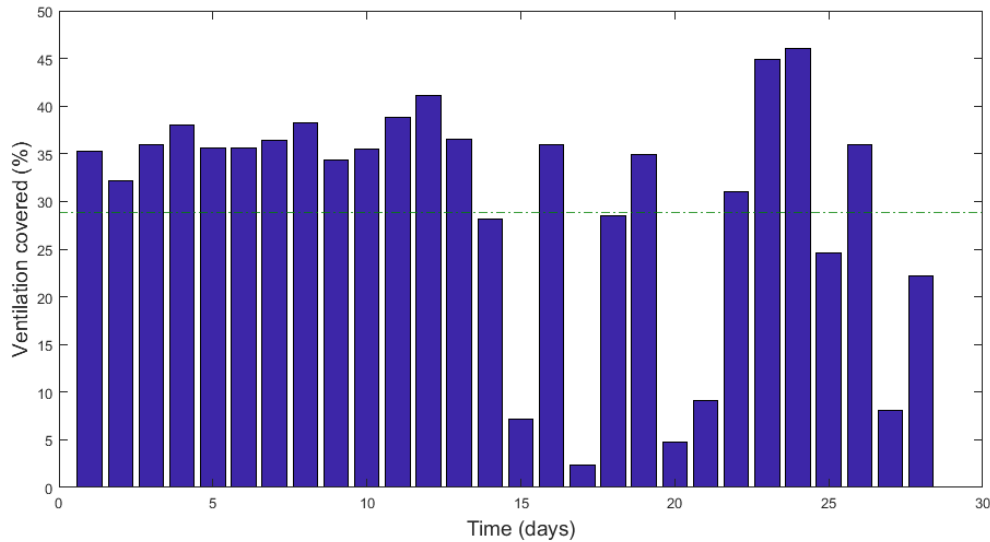


Figure 18. Percentage of daily ventilation covered by the UTC in the experimental tests.

310

311

312

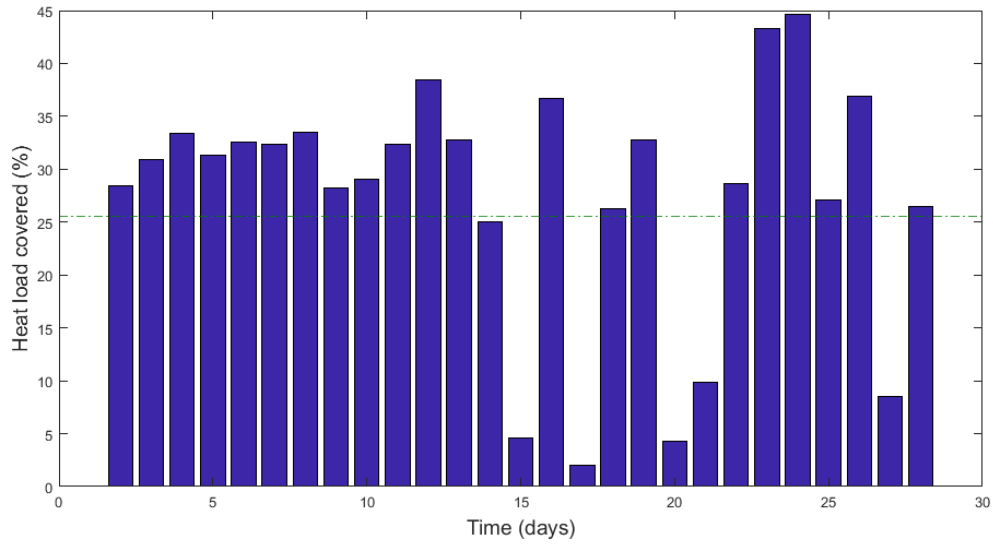
313 3.4 Case study results

314 Figures 18 and 19 show the fraction of ventilation requirements and ventilation heating load covered
 315 by the UTC module tested if it were connected to the ventilation system of the apartment described
 316 in section 2. During sunny days, when the UTC fan is running, the ventilation covered between 28
 317 and 46 % of the ventilation requirements. During cloudy days, these values were between 3 and 10%.
 318 The mean value for the 28 days of tests (green dashed line) was 28 %. As for the ventilation heating
 319 load covered, values reached a maximum of 44 % during sunny days and minimum of 2% during
 320 cloudy days, with a mean value of 26 % for the 28 days of tests. With these data, the minimum area
 321 needed to accomplish the ventilation requirements and to cover the ventilation heating load were
 322 evaluated and represented in figures 20 and 21 as cumulative distribution functions. The expected
 323 area for daily ventilation to cover 100 % of the ventilation requirements was 13.68 m², which
 324 corresponded with up to 80 % of the cases. To cover the ventilation heating load, the expected area
 325 was greater, 15.80 m², and it covered 100 % of the heating required by up to 75 % of the cases.

326 For this case study, the length of façade available to install UTC modules is 9.5 m, so 9 UTC modules
 327 could be installed, giving a total UTC façade area of 20.4 m². With this area, it can be seen in figures
 328 20 and 21 that the percentage of days in which ventilation and ventilation heating could be covered
 329 during the period of the experiments would be 82.2% and 74.8 %, respectively. Therefore, it can be
 330 concluded that for a typical apartment, the reduction in energy consumption when installing a UTC
 331 façade in this climate is considerable.

332

333



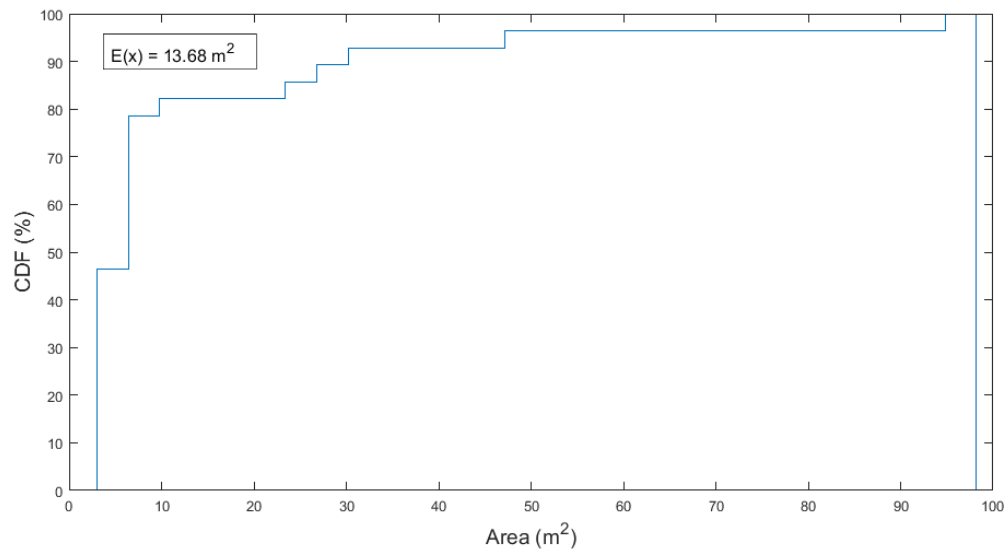
334

335

Figure 19. Percentage of daily ventilation heating covered by the UTC.

336

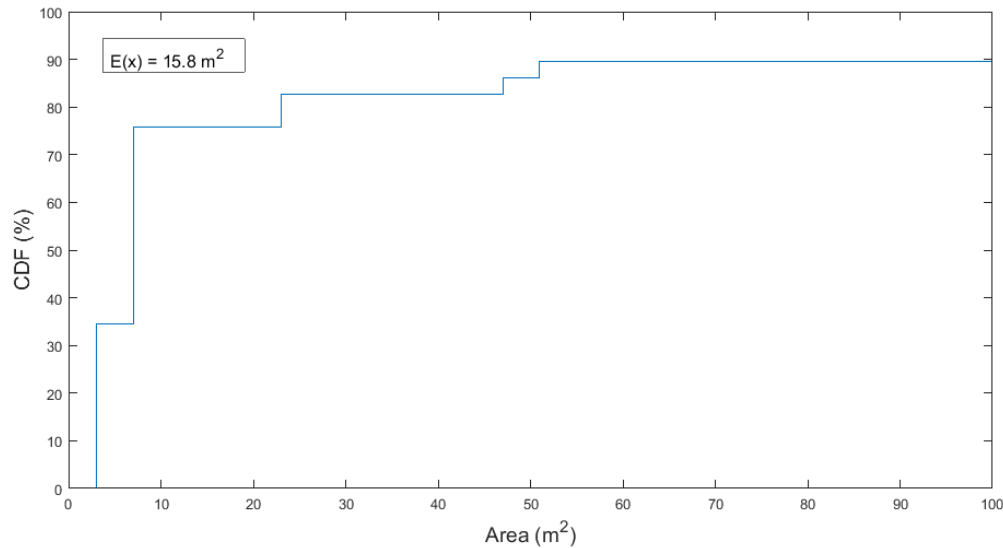
337



338

339

Figure 20. Cumulative distribution function for the UTC surface needed to cover ventilation requirements.



340

341

Figure 21. Cumulative distribution function of the UTC façade surface needed to cover the ventilation heating load.

342

4. Conclusions

343

A module of a UTC façade was tested under ambient weather conditions and the measurements obtained were analysed. With these data, the number of UTC modules needed in a typical apartment to cover the ventilation flow rate and heat load was estimated.

344

345

346

Values of effectivity and effectiveness agreed with those found in other experimental studies. Therefore, the prototype proposed could be viable as a façade solar collector, although an optimisation of the geometry would be needed. The variation in efficiency and effectiveness with solar radiation and temperature was studied. It was found that effectiveness decreased slightly with an increase in ambient temperature, and it increased with an increase in global radiation. Efficiency decreased with an increase in ambient temperature and converged to a common value when the global radiation reached its maximum values.

347

348

349

350

351

352

353

High heating COP values were found when solar radiation and ambient temperatures were high. This corresponded to the most favourable scenario with sunny days with mild winter temperatures. The temperature increase inside the UTC rose with solar radiation, and was less and less dependent on ambient temperature as the solar radiation reached its maximum values.

354

355

356

357

In the case study, it was found that in a typical apartment with the façade orientated to the south, the UTC modules that can be installed would cover a high percentage of the ventilation and heating demand. Therefore, in this location and climate, the use of UTC façades for ventilation and heating was found to be feasible.

358

359

360

361

Further research would be necessary to assess the performance of several modules installed in combination. Two different approaches could be used for module connection: a complete modular approach where each module is provided with its own fan, and a global approach where the modules are connected to a single fan that provides ventilation to all of them. Both approaches need their own control strategy, each having a different performance.

362

363

364

365

366

367

5. Acknowledgements

368 This research was funded by the UCO-SOCIAL-INNOVA program of the Office for Research
369 Transference of the University of Cordoba.

370

371 References

372

373 Al-damook, Amer, and Wissam Hashim Khalil. 2017. "Experimental Evaluation of an Unglazed Solar
374 Air Collector for Building Space Heating in Iraq." *Renewable Energy* 112: 498–509.
375 <https://doi.org/https://doi.org/10.1016/j.renene.2017.05.051>.

376 Badache, Messaoud, Stéphane Hall, and Daniel Rousse. 2012. "A Full 3 4 Factorial Experimental
377 Design for Efficiency Optimization of an Unglazed Transpired Solar Collector Prototype." *Solar*
378 *Energy* 86 (9): 2802–10. <https://doi.org/10.1016/j.solener.2012.06.020>.

379 Badescu, Viorel, Adrian Ciocanea, Sanda Budea, and Iuliana Soriga. 2019. "Regularizing the
380 Operation of Unglazed Transpired Collectors by Incorporating Phase Change Materials."
381 *Energy Conversion and Management* 184 (March): 681–708.
382 <https://doi.org/10.1016/j.enconman.2019.01.049>.

383 Brown, Catherine, Emmanouil Perisoglou, Richard Hall, and Vicki Stevenson. 2014. "Transpired
384 Solar Collector Installations in Wales and England." *Energy Procedia* 48: 18–27.
385 <https://doi.org/10.1016/j.egypro.2014.02.004>.

386 "Código Técnico de La Edificación (CTE) Documento HS 3 - Calidad de Aire Interior." 2017.
387 Ministerio de Fomento. Gobierno de España. <https://www.codigotecnico.org>.

388 Collins, Michael R., and Hani Abulkhair. 2014. "An Evaluation of Heat Transfer and Effectiveness for
389 Unglazed Transpired Solar Air Heaters." *Solar Energy* 99: 231–45.
390 <https://doi.org/10.1016/j.solener.2013.11.012>.

391 Cordeau, Sébastien, and Suzelle Barrington. 2011. "Performance of Unglazed Solar Ventilation Air
392 Pre-Heaters for Broiler Barns." *Solar Energy* 85 (7): 1418–29.
393 <https://doi.org/10.1016/j.solener.2011.03.026>.

394 Decker, G. W E Van, K. G T Hollands, and A. P. Brunger. 2001. "Heat-Exchange Relations for
395 Unglazed Transpired Solar Collectors with Circular Holes on a Square or Triangular Pitch."
396 *Solar Energy* 71 (1): 33–46. [https://doi.org/10.1016/S0038-092X\(01\)00014-7](https://doi.org/10.1016/S0038-092X(01)00014-7).

397 Fleck, B A, R M Meier, and M D Matovic. 2002. "A Field Study of the Wind Effects on the
398 Performance of an Unglazed Transpired Solar Collector." *Solar Energy* 73 (3): 209–16.
399 www.elsevier.com.

400 Gagliano, Antonio, Stefano Aneli, and Francesco Nocera. 2019. "Analysis of the Performance of a
401 Building Solar Thermal Façade (BSTF) for Domestic Hot Water Production." *Renewable Energy*
402 142: 511–26. <https://doi.org/https://doi.org/10.1016/j.renene.2019.04.102>.

403 Giovanardi, A, A Passera, F Zottele, and R Lollini. 2015. "Integrated Solar Thermal Façade System for
404 Building Retrofit." *Solar Energy* 122: 1100–1116.
405 <https://doi.org/https://doi.org/10.1016/j.solener.2015.10.034>.

406 Hall, Richard, and John Blower. 2016. "Low-Emissivity Transpired Solar Collectors." *Energy Procedia*
407 91: 56–63. <https://doi.org/https://doi.org/10.1016/j.egypro.2016.06.171>.

408 Hollick, J. C. 1996. "World's Largest and Tallest Solar Recladding." *Renewable Energy* 9 (1–4): 703–7.
409 [https://doi.org/10.1016/0960-1481\(96\)88382-0](https://doi.org/10.1016/0960-1481(96)88382-0).

- 410 Kassai, Miklos, L Poleczky, Laith Alhyari, László Kajtár, and Jozsef Nyers. 2018. "Investigation of the
411 Energy Recovery Potentials in Ventilation Systems in Different Climates." *Facta Universitatis,*
412 *Series: Mechanical Engineering* 16 (August): 203–17.
413 <https://doi.org/10.22190/FUME180403017K>.
- 414 Kutscher, C F, C B Christensen, and G M Barker. 1993. "Unglazed Transpired Solar Collectors: Heat
415 Loss Theory." *Journal of Solar Energy Engineering* 115 (3): 182–88.
416 <http://dx.doi.org/10.1115/1.2930047>.
- 417 Leon, M Augustus, and S Kumar. 2007. "Mathematical Modeling and Thermal Performance Analysis
418 of Unglazed Transpired Solar Collectors." *Solar Energy* 81 (1): 62–75.
419 <https://doi.org/https://doi.org/10.1016/j.solener.2006.06.017>.
- 420 Love, Chris D., Sanjay B. Shah, Jesse L. Grimes, and Daniel W. Willits. 2014. "Transpired Solar
421 Collector Duct for Tempering Air in North Carolina Turkey Brooder Barn and Swine Nursery."
422 *Solar Energy* 102: 308–17. <https://doi.org/10.1016/j.solener.2013.11.028>.
- 423 Moon, Byeong Eun, Min Ho Lee, Hee Tae Kim, Tae Hyun Choi, Young Bok Kim, Young Sun Ryou, and
424 Hyeon Tae Kim. 2017. "Evaluation of Thermal Performance through Development of an
425 Unglazed Transpired Collector Control System in Experimental Pig Barns." *Solar Energy* 157:
426 201–15. <https://doi.org/10.1016/j.solener.2017.08.026>.
- 427 Peci, F, F Comino, and M Ruiz de Adana. 2018. "Performance of an Unglazed Transpire Collector in
428 the Façade of a Building for Heating and Cooling in Combination with a Desiccant Evaporative
429 Cooler." *Renewable Energy*. <https://doi.org/https://doi.org/10.1016/j.renene.2018.01.029>.
- 430 Peci, F, F Táboas, M Ruiz de Adana, and F Comino. 2019. "Experimental Study of Overheating of an
431 Unglazed Transpired Collector Façade under Southern European Summer Conditions for Four
432 Modes of Operation." *Solar Energy* 189: 194–206.
433 <https://doi.org/https://doi.org/10.1016/j.solener.2019.07.058>.
- 434 Pesaran, Ahmad A., and Keith B. Wipke. 1994. "Use of Unglazed Transpired Solar Collectors for
435 Desiccant Cooling." *Solar Energy* 52 (5): 419–27. [https://doi.org/10.1016/0038-](https://doi.org/10.1016/0038-092X(94)90119-M)
436 [092X\(94\)90119-M](https://doi.org/10.1016/0038-092X(94)90119-M).
- 437 Vasan, Neetha, and Theodore Stathopoulos. 2014. "Experimental Study of Wind Effects on
438 Unglazed Transpired Collectors." *Solar Energy* 101: 138–49.
439 <https://doi.org/https://doi.org/10.1016/j.solener.2013.11.037>.
- 440